Hydrodynamic modeling of electron transport in silicon quantum wires

IOP Conf. Series: Journal of Physics: Conf. Series **906** (2017) 012010 doi:10.1088/1742-6596/906/1/012010

Hydrodynamic modeling of electron transport in silicon quantum wires

O Muscato[1], T Castiglione [1], A Coco [2]

[1] Department of Mathematics and Computer Science, University of Catania, Viale A. Doria 6, Catania 95125, Italy

[2] Department of Mechanical Engineering and Mathematical Sciences, Oxford Brookes University, Wheatley campus, OX33 1HX Oxford GB

E-mail: orazio.muscato@unict.it

Abstract. An extended hydrodynamic model self-consistently coupled to the 2D Schrödinger and 3D Poisson equations is introduced, to describe charge transport in Silicon Nanowires. It is been formulated by taking the moments of the multisubband Boltzmann equation, and the closure relations for the fluxes and production terms have been obtained by means of the Maximum Entropy Principle. The low-field mobility for a Gate-All-Around in a SiNW transistor has been evaluated.

1. Introduction

In the last years, the peculiar electro-thermal properties of silicon nanostructures, have attracted an increasing interest because of the potential applications as sensors, field effect transistors, logic gates, thermoelectric generators [1, 2]. Silicon nanowires (SiNWs) are quasi-one-dimensional structures in which electrons are spatially confined in two directions and they are free to move in the orthogonal direction. By shrinking the dimension of these structures, effects of quantum confinement are observed and the wave nature of the electrons must be taken into account. The investigation of these devices by means of numerical simulations can be very informative, provided that a realistic and complete physical model is employed. Under reasonable hypothesis, transport in low-dimension semiconductors can be tackled coupling quantum and semiclassical tools. Therefore, for long channels, semiclassical formulations based on the 1-D Multiband Boltzmann Transport Equation (MBTE) can give reliable simulation results when it is solved self-consistently with the 3-D Poisson and 2-D Schrödinger equations in order to obtain the self-consistent potential and subband energies. We notice that this semiclassical formulation fails if in the channel there are potential barriers: in this case tunneling effects must be taken into account using quantum kinetic or hydrodynamic models [3, 4].

The Monte Carlo method provides a stochastic solution of the MBTE, although affected by statistical noise [3, 5–10]. Another alternative is to take the moments of the MBTE to obtain hydrodynamic-like models, providing a good engineering-oriented approach. Such approach has been successfully used in the electrical and electro-thermal [11–20] simulation of sub-micrometric electronic devices.

2. Quantum confinement and electronic transport

In SiNW the band structure is altered with respect to the bulk case, depending on the cross-section wire dimension, the atomic configuration, and the crystal orientation. Tight-binding (TB) calculations shows that the six equivalent Δ conduction valleys of the bulk Si are split into two groups because of the quantum confinement [21]. The subbands related to the four **unprimed** valleys Δ_4 ($[0 \pm 10]$ and $[00 \pm 1]$ orthogonal to the wire axis) are projected into a unique valley in the Γ point of the one-dimensional Brillouin zone. Therefore a SiNW is a direct band-gap semiconductor. The subbands related to the **primed** valleys Δ_2 ($[\pm 100]$ along the wire axis) are found at higher energies and exhibit a minimum, located at $k_x = \pm 0.37\pi/a_0$, and the energy gap between the Δ_4 and Δ_2 bottom valley is 117 meV. The corresponding effective masses m^*, in the parabolic spherical band approximation , are $m^*_{\Delta_2} = 0.94$, $m^*_{\Delta_4} = 0.27$ (in rest electron mass units). For a quantum wire with linear expansion in x-direction, and confined in the plane $y - z$, the normed wave function $\phi(x, y, z)$ can be written in the form

$$\phi(x, y, z) = \chi^{\mu}_{l}(y, z)\frac{e^{ik_x x}}{\sqrt{L_x}} \tag{1}$$

where μ is the valley index (one Δ_4 valley and two Δ_2 valleys), $l = 1, N_{sub}$ the subband index, $\chi^{\mu}_{l}(y, z)$ is the wave function of the l-th subband and μ-th valley, and the term $e^{ik_x x}/\sqrt{L_x}$ describes an independent plane wave in x-direction confined to the normalization length, $0 \leq x \leq L_x$, with wave number k_x. In the Hartree approximation, a given electron feels the total potential $V_{tot}(x, y, z) = U(y, z) - eV(x, y, z)$, where V is the electrostatic potential, e is the absolute value of the electric charge, and $U(y, z)$ the confining potential. The spatial confinement in the (y, z) plane is governed by the Schrödinger-Poisson system (SP)

$$\begin{cases} H[V]\,\chi^{\mu}_{lx}[V] = \varepsilon^{\mu}_{lx}[V]\,\chi^{\mu}_{lx}[V] \\ \\ H[V] = -\dfrac{\hbar^2}{2m^*_{\mu}}\left(\dfrac{\partial^2}{\partial y^2} + \dfrac{\partial^2}{\partial z^2}\right) + V_{tot}(x, y, z) \\ \\ \nabla \cdot [\epsilon_0 \epsilon_r \nabla V(x, y, z)] = -e(N_D - N_A - n[V]) \\ \\ n[V](x, y, z, t) = \sum_{\mu}\sum_{l} \rho^{\mu}_{l}(x, t)|\chi^{\mu}_{lx}[V](y, z, t)|^2 \end{cases} \tag{2}$$

where $(2)_1$ is the Schrödinger equation in the Effective Mass Approximation, $(2)_3$ is the Poisson equation, and N_D, N_A are the assigned doping profiles (due to donors and acceptors). The electron density $n[V]$ is given by $(2)_4$, where $\rho^{\mu}_{l}(x, t)$ is the linear density in the μ-valley and l-subband which must be evaluated by the transport model (hydrodynamic/kinetic) in the free movement direction. In the following we shall assume a quadratic cross-section of the wire (having total dimension $L_y = L_z$) where the wire is surrounded by an oxide layer which gives rise to a deep potential barrier having $U = 4.05$ eV. The SP system forms a coupled nonlinear PDEs, which it is usually solved by using an adaptive iteration scheme, obtaining the electrostatic potential V, the eigenvalues (or subband energies) ε^{μ}_{lx}, and the eigenvectors (or electron envelope wavefunctions) χ^{μ}_{lx} as a function of the unconfined x direction. Then the total electron energy in the μ-valley and l-subband is $E^{\mu}_{l} = \varepsilon^{\mu}_{lx} + \dfrac{\hbar^2 k_x^2}{2m^*_{\mu}}$.

The electrons evolve in time under the streaming motion of external forces and spatial gradient, and the randomizing influence of nearly point-like (in space-time) scattering events.

For devices with a characteristic length of a few tens of nanometers, the transport of electrons along the axis of the wire can be considered semiclassical within a good approximation [22], and it can be modeled by the 1D MBTE. By taking moments of the MBTE, the following extended hydrodynamic model [23–25] has been obtained

$$\frac{\partial \rho_l^\mu}{\partial t} + \frac{\partial(\rho_l^\mu V_l^\mu)}{\partial x} = \rho_l^\mu \sum_{l'} \mathcal{C}_\rho(\mu,l,\mu,l') + \rho_l^\mu \sum_{l',\mu'\neq\mu} \mathcal{C}_\rho(\mu,l,\mu',l') \tag{3}$$

$$\frac{\partial(\rho_l^\mu V_l^\mu)}{\partial t} + \frac{2}{m_\mu^*}\frac{\partial(\rho_l^\mu W_l^\mu)}{\partial x} + \frac{\rho_l^\mu}{m_\mu^*}\frac{\partial \varepsilon_l^\mu}{\partial x} = \rho_l^\mu \sum_{l'} \mathcal{C}_V(\mu,l,\mu,l') + \rho_l^\mu \sum_{l',\mu'\neq\mu} \mathcal{C}_V(\mu,l,\mu',l') \tag{4}$$

$$\frac{\partial(\rho_l^\mu W_l^\mu)}{\partial t} + \frac{\partial(\rho_l^\mu S_l^\mu)}{\partial x} + \rho_l^\mu \frac{\partial \varepsilon_l^\mu}{\partial x} V_l^\mu = \rho_l^\mu \sum_{l'} \mathcal{C}_W(\mu,l,\mu,l') + \rho_l^\mu \sum_{l',\mu'\neq\mu} \mathcal{C}_W(\mu,l,\mu',l') \tag{5}$$

$$\frac{\partial(\rho_l^\mu S_l^\mu)}{\partial t} + \frac{\partial(\rho_l^\mu F_l^\mu)}{\partial x} + \frac{3\rho_l^\mu}{m_\mu^*}\frac{\partial \varepsilon_l^\mu}{\partial x} W_l^\mu = \rho_l^\mu \sum_{l'} \mathcal{C}_S(\mu,l,\mu,l') + \rho_l^\mu \sum_{l',\mu'\neq\mu} \mathcal{C}_S(\mu,l,\mu',l') \tag{6}$$

where (3)-(6) represent balance equations for the density (ρ_l^μ), momentum (V_l^μ), energy (W_l^μ) and energy-flux (S_l^μ) respectively. This system is not closed due the presence of the high-order moment F_l^μ as well as of the production terms (i.e. the RHS). By using the Maximum Entropy Principle [26–29], one determines functional form of the distribution function in a neighborhood of local thermal equilibrium, and consequently in [24], we have obtained $F_l^\mu = 6(W_l^\mu)^2/m_\mu^*$ and the terms $\mathcal{C}_\rho, \mathcal{C}_V, \mathcal{C}_W, \mathcal{C}_S$, which have been calculated taking into account scattering with acoustic and optical phonons, as well as surface roughness (SR). This model provides a realistic description of the scattering rates, an useful tool to evaluate the low-field mobility and also far-from equilibrium transport regimes.

3. Simulation results

We have considered a Gate-All-Around Silicon Nanowire transistor (SiNWT) having a parallelepiped geometry with a metal gate wrapped around it, in such a way we have a three contact device. Such devices have been designed during these years in order to maintain a good electrostatic control in the channel. The channel has been homogeneously doped to $N_D = 3\ 10^{17}\,\mathrm{cm}^{-3}$ and it is very long ($L_x = 120$ nm) with respect to the transversal dimensions ($L_y = L_z = 12$ nm), and the oxide thickness is 1 nm. As preliminary result, we have evaluated the low-field mobility in this long-channel device. In order to evaluate this parameter, we fix an uniform electric field along the channel of 1 kV/cm, and then we compute the mobility as the ratio between the average electron velocity and the driving field, as function of the gate voltage V_g. The average electron velocity has been obtained with the following iterative procedure: i) we fix V_g and solve the Schrödinger-Poisson system (2); ii) once this solution has been obtained, the energies ε_l^μ and wave functions χ_l^μ for each subband are exported into the hydrodynamic model, and the linear density ρ_l^μ is used as initial condition; iii) the hydrodynamic model (3)-(6) is solved and, in the stationary regime, the average velocity has been calculated. In Fig. 1 we plot the electron density in a cross-section of the wire, showing the formation of the surface inversion layer with the electron density peaked close to the oxide interface. In Fig. 2 we show the low-field mobility as function of the gate voltage V_g, obtained by including/excluding the SR mechanism. The inclusion of SR scattering has a strong effect on the low-field mobility dependence, and it is a key point in the simulation of such devices.

□

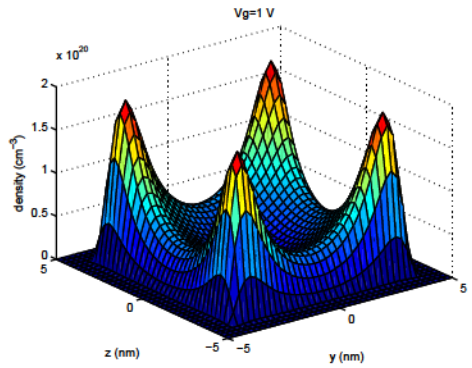

Figure 1. The electron density for $V_g = 1V$ in a wire cross-section.

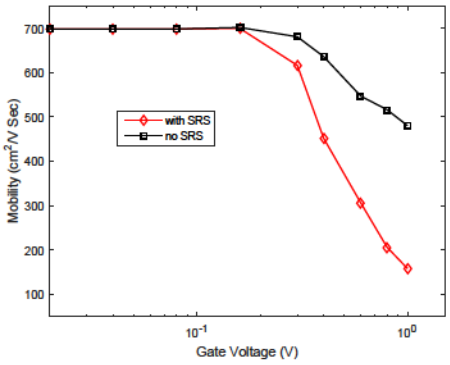

Figure 2. Low-field mobility versus gate voltage, obtained with/without Surface Roughness Scattering mechanism.

Acknowledgments

We acknowledge the support of the Università degli Studi di Catania, FIR 2014 "Charge Transport in Graphene and Low dimensional Structures: modeling and simulation".

References

[1] Pennelli G, Nannini A and Macucci M 2014 *J. Appl. Phys.* **115** 084507
[2] Guerfi Y and Larrieu G 2016 *Nanoscale Res. Lett* **11** 210
[3] Muscato O and Wagner W 2016 *SIAM J. Sci. Comp.* **38** A1483
[4] Gardner C 1994 *SIAM J. Appl. Math.* **54** 409
[5] Lenzi M, Palestri P, Gnani E, Reggiani S, Gnudi A, Esseni D, Selmi L and Baccarani G 2008 *IEEE Trans. elec. Dev.* **55** 2086
[6] Knezevic I, Ramayya E, Vasileska D and Goodnick S 2009 *J. Comput. Theor. Nanosc.* **6** 1725
[7] Ramayya E and Knezevic I 2010 *J. Comput. Electr.* **9** 206
[8] Muscato O, Wagner W and Di Stefano V 2011 *Kinetic Rel. Models* **4** 809
[9] Muscato O, Di Stefano V and Wagner W 2013 *Comput. Math. Appl.* **65** 520
[10] Ryu H 2016 *Nanos. Res.Lett.* **11** 36
[11] Muscato O and Di Stefano V 2011 *J. Phys. A:Math. Theor.* **44** 105501
[12] Muscato O and Di Stefano V 2011 *J. Stat. Phys.* **144** 171
[13] Muscato O and Di Stefano V 2011 *J. Appl. Phys.* **110** 093706
[14] Di Stefano V and Muscato O 2012 *Acta Appl. Math.* **121** 225
[15] Muscato O and Di Stefano V 2013 *Semicond. Sci. Technol.* **28** 025021
[16] Muscato O, Wagner W and Di Stefano V 2014 *COMPEL* **33** 1198
[17] Mascali G 2015 *Eur. J. Appl. Math.* **26** 477
[18] Muscato O and Di Stefano V 2015 *SIAM J. Appl. Math.* **75** 1941
[19] Mascali G 2016 *J. Stat. Phys.* **163** 1268
[20] Mascali G 2017 *J. Comput. Electr.* **16** 180
[21] Zheng Y, Rivas C, Lake R, Alam K, Boykin T and Klimeck G 2005 *IEEE Trans. Elec. Dev.* **52** 1097
[22] Ferry D, Goodnick S and Bird J 2009 *Transport in Nanostructures* (Cambridge: Cambridge Univ. Press)
[23] Muscato O and Castiglione T 2016 *Comm. Appl. Industr. Math.* **7** 8
[24] Muscato O and Castiglione T 2016 *Entropy* **18** 368
[25] Castiglione T and Muscato O 2017 *J. Comput. Theor. Transp.* **46** 186
[26] Camiola V, Mascali G and Romano V 2012 *Contin. Mech. Thermodyn.* **24** 417
[27] Muscato O and Di Stefano V 2012 *J. Comp. Electr.* **11** 45
[28] Camiola V, Mascali G and Romano V 2013 *Math. Comput. Mod.* **58** 321
[29] Muscato O and Di Stefano V 2014 *Contin. Mech. Thermodyn.* **26** 197

□